

Biochemical and Clinical Predictive Approach and Time Point Analysis of Hepatobiliary Phase Liver Enhancement on Gd-EOB-DTPA-enhanced MR Images: A Multicenter Study¹

Masahiro Okada, MD, PhD
Takamichi Murakami, MD, PhD
Ryohei Kuwatsuru, MD, PhD
Yuko Nakamura, MD, PhD
Hiroyoshi Isoda, MD, PhD
Satoshi Goshima, MD, PhD
Ryota Hanaoka, MD, PhD
Hiroki Haradome, MD, PhD
Yoshinobu Shinagawa, MD, PhD
Azusa Kitao, MD, PhD
Yasunari Fujinaga, MD, PhD
Nagaaki Marugami, MD, PhD
Masako Yuki, MD, PhD
Tomoaki Ichikawa, MD, PhD
Atsushi Higaki, MD, PhD
Masatoshi Hori, MD, PhD
Shinya Fujii, MD, PhD
Osamu Matsui, MD, PhD

Purpose:

To identify biochemical factors associated with liver enhancement over time on gadolinium ethoxybenzyl diethylenetriamine pentaacetic acid (Gd-EOB-DTPA)-enhanced magnetic resonance (MR) images and predict the optimal time point of the hepatobiliary phase in various clinical settings.

Materials and Methods:

This study was approved by the institutional review boards, and written informed consent was obtained from the 1903 patients enrolled. Simple and multiple logistic regression analyses were performed to investigate the biochemical factors associated with liver-to-spleen contrast (LSC) of at least 1.5 in the hepatobiliary phase. Changes in LSC and lesion-to-liver contrast (LLC) of lesions over time (at 5, 10, 15, and 20 minutes) were investigated with a linear mixed-effects model in patients and lesions. For LSC, the optimal cutoff value was determined with receiver operating characteristic analysis of the most significant variable. Differences in LSC and LLC were analyzed in various clinical settings.

Results:

Ultimately, 1870 patients were evaluated, as 33 were excluded according to study criteria. Prothrombin (PT) activity, total bilirubin level ($P = .020$), and total cholesterol level ($P = .005$) were significantly associated with LSC of at least 1.5 at 20 minutes, and PT activity was identified as the most significant factor (odds ratio, 1.271; 95% confidence interval: 1.109, 1.455; $P = .001$). LSC of at least 1.5 at 20 minutes with PT activity of at least 86.9% and less than 86.9% occurred in 555 of 626 patients (88.6%) and 388 of 575 patients (67.5%), respectively. Satisfactory liver enhancement at 20 minutes was significantly more likely to be achieved by patients with hepatitis B virus than by those with hepatitis C virus ($P < .001$) and by patients with metastasis than by those with hepatocellular carcinoma ($P < .001$). No significant difference in LLC was observed in patients examined at 1.5 and 3.0 T ($P = .133$).

Conclusion:

Hepatic enhancement is significantly associated with PT activity, total bilirubin level, and total cholesterol level. PT activity of at least 86.9% could be used to shorten examination times at Gd-EOB-DTPA-enhanced MR imaging.

© RSNA, 2016

Online supplemental material is available for this article.

¹From the Department of Radiology, Kinki University Faculty of Medicine, Osaka, Japan (M.O., T.M.). The complete list of author affiliations is listed at the end of this article. Received May 9, 2015; revision requested July 2; revision received December 27; accepted February 2, 2016; final version accepted March 16. Address correspondence to M.O., Department of Radiology, University of the Ryukyus, 207 Nishihara, Okinawa 903-0215, Japan (e-mail: mokada@gaia.eonet.ne.jp).

Supported by Bayer Yakuhin, Osaka, Japan.

© RSNA, 2016

Gadolinium ethoxybenzyl diethylenetriamine pentaacetic acid (Gd-EOB-DTPA) is a hepatic-specific magnetic resonance (MR) contrast agent that shows extracellular distribution and hepatocyte selective uptake during the hepatobiliary phase (1,2). It is useful for detecting hepatocellular carcinoma (HCC) and liver metastasis (3). Moreover, the degree of hepatic enhancement during the hepatobiliary phase reflects the level of liver function (4,5). Patients with cirrhotic livers may show reduced

signal intensity in the hepatobiliary phase because patients with Child-Pugh class B or C disease have been shown to demonstrate decreased liver enhancement as measured with T1 and T2* relaxation times (5,6). Kim et al reported in their animal study that decreased liver enhancement was related to prolonged prothrombin (PT) time and indocyanine green half-life and increased bilirubin level (7). Motosugi et al reported that in patients who had Child-Pugh class B and C disease, delayed indocyanine green retention rate at 15 minutes (ICG-R15) was significantly correlated with unsatisfactory Gd-EOB-DTPA liver enhancement in the hepatobiliary phase (8). Some other reports showed that poor liver enhancement on Gd-EOB-DTPA-enhanced MR images was correlated with increased Model for End Stage Liver Disease sodium score, hypoalbuminemia, or ascites (9); decreased PT activity, hyperbilirubinemia, hypoalbuminemia, delayed ICG-R15, and thrombopenia (10); and increased aspartate aminotransferase (AST) level and hyperbilirubinemia (11). However, only a small number of patients were retrospectively evaluated in these studies.

The objective of this multicenter study was to identify biochemical factors and other clinical and technical factors associated with liver enhancement (liver-to-spleen contrast [LSC]) and lesion-to-liver contrast (LLC) over time on Gd-EOB-DTPA-enhanced MR images and predict the optimal time point of the hepatobiliary phase in various clinical settings.

Materials and Methods

As a funding source, this study was supported by Bayer Yakuhin (Osaka, Japan),

Implication for Patient Care

- PT activity of at least 86.9% could be used to shorten examination time on Gd-EOB-DTPA-enhanced MR images, because estimated means of LSC in PT activity of at least 86.9% at 5, 10, 15, and 20 minutes were 1.548 (95% CI: 1.492, 1.604), 1.741 (95% CI: 1.695, 1.787), 1.920 (95% CI: 1.878, 1.962), and 2.045 (95% CI: 2.008, 2.081), respectively.

which had no role regarding the study performance. This study was approved by the institutional review boards. Written informed consent for the use of database images and biochemical factors was obtained. Moreover, our study was officially registered in the Clinical Trials Registry of University Hospital Medical Information Network (no. 000008229).



Patients

Forty-five hospitals participated in this retrospective review of prospectively acquired data. A total of 1903 consecutive patients underwent Gd-EOB-DTPA-enhanced MR imaging between January 2012 and July 2013. Inclusion criteria were serum creatinine level more than the upper normal limit (estimated glomerular filtration rate ≥ 30 mL/min/1.73 m²), body weight less than 100 kg, clear level of consciousness, and age range of 20–84 years. Exclusion criteria were contraindications to MR imaging, such as having a pacemaker, a history of hypersensitivity to gadolinium-based contrast agents, bronchial asthma or severe allergic disease, severe renal

Advances in Knowledge

- Satisfactory liver enhancement 20 minutes after gadolinium ethoxybenzyl diethylenetriamine pentaacetic acid (Gd-EOB-DTPA) injection was significantly associated with prothrombin (PT) activity ($P = .001$), total bilirubin level ($P = .020$), and total cholesterol level ($P = .005$).
- Liver-to-spleen contrast (LSC, the signal intensity ratio of liver to spleen) was significantly higher in patients with PT activity of at least 86.9% than in those with PT activity less than 86.9% at 5 minutes ($P < .001$), 10 minutes ($P < .001$), 15 minutes ($P < .001$), and 20 minutes ($P < .001$) at a significance level of .0125 after an injection of Gd-EOB-DTPA.
- Twenty minutes after injection, 88.7% (95% confidence interval [CI]: 85.9%, 91.0%) of patients with PT activity of at least 86.9% had satisfactory liver enhancement (LSC ≥ 1.5), whereas 67.5% (95% CI: 63.5%, 71.3%) of patients with PT activity less than 86.9% had satisfactory liver enhancement.
- Patients with hepatocellular carcinoma (HCC) were significantly less likely to achieve LSC of at least 1.5 than those with liver metastasis at 20 minutes (odds ratio, 0.323; 95% CI: 0.199, 0.524; $P < .001$).
- Lesion-to-liver contrast (the signal intensity ratio of lesion to liver) was significantly lower in patients with HCC than in those with borderline lesions at 5 minutes ($P = .0002$), 10 minutes ($P < .0001$), 15 minutes ($P < .0001$), and 20 minutes ($P < .0001$) at a significance level of P less than .00125.

Published online before print

10.1148/radiol.2016151061 Content codes:  

Radiology 2016; 281:474–483

Abbreviations:

ALT = alanine aminotransferase
 AST = aspartate aminotransferase
 CI = confidence interval
 Gd-EOB-DTPA = gadolinium ethoxybenzyl diethylenetriamine pentaacetic acid
 HBV = hepatitis B virus
 HCC = hepatocellular carcinoma
 HCV = hepatitis C virus
 ICG-R15 = indocyanine green retention rate at 15 minutes
 LLC = lesion-to-liver contrast
 LSC = liver-to-spleen contrast
 PT = prothrombin

Author contributions:

Guarantors of integrity of entire study, M.O., A.K.; study concepts/study design or data acquisition or data analysis/interpretation, all authors; manuscript drafting or manuscript revision for important intellectual content, all authors; approval of final version of submitted manuscript, all authors; agrees to ensure any questions related to the work are appropriately resolved, all authors; literature research, M.O., T.M., R.K., S.G., H.H., Y.S., Y.F., A.H., M.H., O.M.; clinical studies, all authors; statistical analysis, M.O.; and manuscript editing, M.O., T.M., T.I., O.M.

Conflicts of interest are listed at the end of this article.

dysfunction, current pregnancy, and current lactation. Clinical laboratory data were obtained within 1 month before Gd-EOB-DTPA-enhanced MR imaging.

Gd-EOB-DTPA was intravenously injected at a dose of 25 μ mol per kilogram of body weight (0.1 mL/kg) with several injection methods and speeds (Appendix E1 [online]). In all institutions, three-dimensional T1-weighted images with fat suppression were acquired for hepatobiliary phase imaging (1.5-T Gyroscan Intera Nova [Philips Medical Systems, Best, the Netherlands], with repetition time msec/echo time msec of 4.4/2.2, flip angle of 10°, sensitivity encoding factor of 1.8, section thickness of 5 mm, section interval of 2.5 mm, matrix of 320 \times 512 \times 2.50 mm, and field of view of 375 mm; and 3.0-T Achieva [Philips], with 3.5/1.7, flip angle of 10°, sensitivity encoding factor of 1.9, section thickness of 3 mm, section interval of 1.5 mm, matrix of 512 \times 512 \times 1.50 mm, and field of view of 350 mm). Background liver diseases were recorded in each hospital.

Biochemical Factors

Biochemical factors investigated were as follows. In most patients (Tables 1, 2), AST level, ALT level, albumin level, total bilirubin level, PT activity, and Child-Pugh classification were available. In addition, total protein level, alkaline phosphatase level, γ -glutamyl transpeptidase level, lactate dehydrogenase level, γ -globulin level, blood urea nitrogen level, serum creatinine level, total cholesterol level, prothrombin time, and ICG-R15 were also available in some patients.

Image Analysis

An example of the MR imaging technique of three-dimensional T1-weighted imaging in the hepatobiliary phase is shown in Appendix E1 (online). The hepatic and tumor enhancement and size were measured in the hepatobiliary phase, but these were not analyzed in the vascular phases. LSC and LLC at each time point were evaluated by one of the investigators (M.O., T.M., R.K., Y.N., H.I., S.G., R.H., H.H., Y.S., A.K., Y.F., N.M., M.Y., T.I., A.H., M.H., and S.F., each with more than 8 years of

experience in abdominal imaging) at each hospital. The signal intensity of the liver was defined on the contrast-enhanced three-dimensional T1-weighted images as the mean signal intensity from four divided segments (anterior and posterior segments of the right hepatic lobe and medial and lateral segments of the left hepatic lobe). At each institution, we measured signal intensity of the liver by using an operator-defined region of interest 10–15 mm in diameter, which was placed by avoiding visible vascular structures and tumors. Two regions of interest (10–15 mm in diameter) were placed in the spleen.

LSC was defined as hepatic signal intensity divided by splenic signal intensity, and satisfactory liver enhancement was defined as LSC of at least 1.5, in accordance with a previous study (8).

One area of the liver tumor was used for the measurement of signal intensity of the tumor, and LLC was defined as tumor signal intensity divided by hepatic signal intensity. For one patient, larger regions of interest inside of a maximum of six tumors (mean, 1.7 tumors per patient), which showed low or high signal intensity of the tumor compared with surrounding liver, were measured so as not to run off the edge of the tumors (region of interest of 2–25 mm in diameter).

The relation between biochemical factors and LSC of at least 1.5 at 20 minutes and the changes in LSC of patients and LLC of lesions were analyzed. In addition, the effect of magnetic field strength (1.5 T or 3.0 T) and the association of disease origins (hepatitis B virus [HBV], hepatitis C virus [HCV], HCC, or liver metastasis) were analyzed.

Standard of Reference in Diagnosis

In the diagnosis of liver tumors, the standard of reference was a combination of liver resection ($n = 60$); typical imaging features for the diagnosis of HCC on ultrasonographic, computed tomographic, or MR images according to the American Association for the Study of Liver Diseases guidelines (12); and/or follow-up images for lesion characterization ($n = 914$ for the sum of American Association for the Study of

Liver Diseases characteristics and follow-up). The follow-up interval was set for a minimum of 6 months. When a hypovascular solid nodule was found in a patient at high risk for HCC, and when the possibility of finding other hypovascular masses (such as liver metastases) was low according to clinical parameters, the nodule was diagnosed as a “borderline lesion” of HCC, which could possibly include dysplastic nodules and pathologic early HCC. Histopathologic findings of the liver specimen (HCC, $n = 33$) and imaging findings with follow-up data (HCC, $n = 455$; borderline lesion, $n = 49$) were used for diagnosis.

Statistical Analysis

Statistical analysis details are given in Appendix E2 (online). The target number of patients was set at 1800 to detect the significance of the odds ratio in multiple logistic regression analysis. Patient characteristics and biochemical variables were summarized as means \pm standard deviations or ranges with interquartile ranges. Biochemical factors associated with LSC of at least 1.5 at 20 minutes were identified with simple and multiple logistic regression analysis. Changes in LSC of patients and LLC of lesions over time were investigated with a linear mixed-effects model. Regarding LSC, patients were stratified according to cutoff values determined at receiver operating characteristic analysis for the most significant variable identified and according to magnetic field intensity (1.5 T or 3.0 T). The association between patient groups (with disease origin of HBV, HCV, HCC, or liver metastasis) and LSC of at least 1.5 at 20 minutes was investigated with logistic regression analysis adjusted for Child-Pugh classification.

Regarding LLC, the diagnoses of lesions and magnetic field intensities were used as lesion-grouping variables. Further analysis was performed in borderline lesions of patients with LSC less than 1.5 at 20 minutes, stratified according to the receiver operating characteristic cutoff value mentioned earlier. The significance level of all the statistical tests was set at an α level of .05. The multiplicity of tests was addressed with the Bonferroni method. SPSS Statistics

Table 1**Patient Characteristics**

Parameter	No. of Patients	Mean*	Minimum Value	Maximum Value	Median Value	1st Quartile	3rd Quartile
Patient age (y)	1870	67 ± 11	20.0	84.0	68.0	61.0	75.0
Men	1186 (63.4)	67 ± 10	20.0	84.0	68.0	61.0	75.0
Women	684 (36.6)	66 ± 12	21.0	84.0	69.0	61.0	75.0
Patient height (cm)	1791	160.8 ± 9.2	124.0	195.0	162.0	154.0	167.0
Men	1142 (63.8)	165.6 ± 6.7	136.0	195.0	165.0	161.1	170.0
Women	649 (36.2)	152.3 ± 6.6	124.0	175.0	152.0	148.0	157.0
Patient weight (kg)	1835	59.8 ± 11.2	30.0	99.0	59.4	52.0	67.0
Men	1165 (63.5)	63.6 ± 10.3	37.3	99.0	63.0	56.2	70.0
Women	670 (36.5)	53.2 ± 9.4	30.0	98.6	52.0	46.8	58.4

Note.—Numbers in parentheses are percentages. The biochemical clinical data were obtained within 1 month before Gd-EOB-DTPA-enhanced MR imaging. There were 1782 patients with Child-Pugh classification: 1447 (81.2%) patients with Child-Pugh class A disease, 308 (17.3%) patients with Child-Pugh class B disease, and 27 (1.5%) patients with Child-Pugh class C disease.

* Data are means ± standard deviations.

Table 2**Baseline Biochemical Values**

Parameter	No. of Patients	Mean*	Minimum Value	Maximum Value	Median Value	1st Quartile	3rd Quartile
AST level (IU/L)	1844	47 ± 50	7.0	831.0	35.0	24.0	57.0
Alanine aminotransferase (ALT) level (IU/L)	1844	41 ± 48	3.0	660.0	28.0	18.0	46.0
Albumin level (g/dL)	1842	4.6 ± 14.4	1.8	432.0	4.0	3.5	4.3
Total bilirubin level (mg/dL)	1840	1.1 ± 1.3	0.03	22.6	0.8	0.6	1.2
PT activity (%)	1770	86.2 ± 19.0	5.3	188.0	88.0	76.0	98.8
Total protein level (g/dL)	1280	7.3 ± 0.67	4.6	9.5	7.3	6.9	7.7
Alkaline phosphatase level (IU/L)	1367	353 ± 242	2.8	4021.0	292.0	227.0	404.0
γ-glutamyl transpeptidase level (IU/L)	1351	92.3 ± 158	3.1	2015.0	43.0	24.0	82.0
Lactate dehydrogenase level (IU/L)	1346	234.3 ± 129.7	2.5	2071	208	180	253
γ-globulin level (mg/dL)	154	161.2 ± 479.2	0.81	2800	3.4	2.9	6.0
Blood urea nitrogen level (mg/dL)	1386	15.0 ± 5.4	0.5	52.0	14.0	11.2	18.0
Serum creatinine level (mg/dL)	1406	0.76 ± 0.21	0.063	1.93	0.73	0.61	0.87
Total cholesterol level (mg/dL)	816	173.1 ± 55.4	1.9	1183	169	146	196
PT time (sec)	1142	14.6 ± 11.2	0.95	131.6	12.6	11.6	13.8
ICG-R15 (%)	166	15.1 ± 12.7	0.0	69.2	12.8	6.4	21.5

Note.—The biochemical factors and clinical data were obtained within 1 month before Gd-EOB-DTPA-enhanced MR imaging. To convert international units per liter to microkatal per liter for AST, ALT, alkaline phosphatase, and lactate dehydrogenase levels, multiply by 0.0167. To convert grams per deciliter to grams per liter for albumin and total protein levels, multiply by 10. To convert milligrams per deciliter to micromoles per liter for total bilirubin level, multiply by 17.104. To convert milligrams per deciliter to millimoles per liter for blood urea nitrogen level, multiply by 0.357. To convert milligrams per deciliter to micromoles per liter for serum creatinine level, multiply by 88.4. To convert milligrams per deciliter to millimoles per liter for total cholesterol level, multiply by 0.0259. Normal ranges are as follows: AST level, 5–37 IU/L; ALT level, 6–43 IU/L; albumin level, 4.0–5.2 g/dL; total bilirubin level, 0.4–1.2 mg/dL; PT activity, 70%–100%; total protein level, 6.6–8.1 g/dL; alkaline phosphatase level, 110–348 IU/L; γ-glutamyl transpeptidase level, 0–75 IU/L; lactate dehydrogenase level, 119–221 IU/L; γ-globulin level, 870–1700 mg/dL; blood urea nitrogen level, 9–21 mg/dL; serum creatinine level, 0.6–1.0 mg/dL for men and 0.5–0.8 mg/dL for women; total cholesterol level, 150–219 mg/dL; PT time, 12–14 seconds; and ICG-R15, 0%–10%.

* Data are means ± standard deviations.

software version 21.0 (IBM, Armonk, NY) was used for statistical analysis.

Results**Patients**

Thirty-three patients were excluded (body weight exceeded the limit, $n = 7$;

age exceeded the limit, $n = 24$; discontinuance of MR examination, $n = 1$; and asthma, $n = 1$) from the 1903 enrolled patients; therefore, the final study population consisted of 1870 patients (1186 men [63.4%] and 684 women [36.6%]). There were 988 hepatic lesions registered. Baseline patient characteristics and biochemical

variables are summarized in Tables 1 and 2.

The underlying liver diseases in these patients were HBV in 289 patients (15.4%), HCV in 716 patients (38.3%), ethanol in 95 patients (5.1%), HBV with HCV in 13 patients (0.7%), primary biliary cirrhosis in eight patients (0.4%), nonalcoholic steatohepatitis in

five patients (0.3%), HCV with ethanol in three patients (0.2%), liver cirrhosis of unknown origin in three patients (0.2%), hemochromatosis in one patient (0.1%), Wilson disease in one patient (0.1%), non-HBV and non-HCV in 585 patients (31.3%), and unknown disease in 151 patients (8.1%). The diagnoses of 988 hepatic lesions are shown in Appendix E3 [online].

Relationship between Satisfactory Liver Enhancement in the Hepatobiliary Phase and Biochemical Factors

The results of simple and multiple logistic regression analyses used to assess associations between biochemical factors and LSC of at least 1.5 at 20 minutes are shown in Tables 3 and 4, respectively. AST ($P < .001$), total bilirubin level ($P < .001$), PT activity ($P < .001$), total cholesterol level ($P < .001$), and Child-Pugh classification ($P < .001$) showed statistically significant associations in simple logistic regression analyses (Table 3). In the best-fit multiple logistic regression model, PT activity ($P = .001$), total bilirubin level ($P = .020$), and total cholesterol level ($P = .005$) showed statistical significance—in particular, the P value of PT activity was the smallest. The odds ratio for a 10-unit increase of PT activity was 1.271 (95% confidence interval [CI]: 1.109, 1.455; Table 4). Receiver operating characteristic analysis yielded the optimal cutoff value of 86.9% for PT activity to predict LSC of at least 1.5 at 20 minutes (area under the curve, 0.693; sensitivity, 0.725; specificity, 0.589).

LSC Values

LSC less than 1.5 and LSC of at least 1.5 were seen in 258 patients (21.5%) and 943 patients (78.5%) among 1201 patients, respectively, who had both PT activity and LSC data measured at 20 minutes. The type III tests of fixed effects in the mixed-effects model showed significant interaction between time and groups (group A, PT activity $\geq 86.9\%$; group B, PT activity $< 86.9\%$), as shown in Figure 1 ($P = .001$). Post hoc comparison showed a significant increase of LSC at 20 minutes in both of the groups ($P < .001$) at a significance level of .00625.

Table 3

Results of Simple Logistic Regression Analyses for Biochemical Factors, Including Child-Pugh Classification

Variable	No. of Patients	<i>P</i> Value*	Odds Ratio†	Adjusted 95% CI
AST level†	1232	<.001	0.920	0.870, 0.972
ALT level†	1232	.010	0.968	0.932, 1.005
Albumin level†	1232	.615	1.040	0.826, 1.309
Total bilirubin level	1228	<.001	0.533	0.399, 0.710
PT activity†	1201	<.001	1.347	1.202, 1.510
Total protein level	891	.899	1.015	0.717, 1.437
Alkaline phosphatase level†	952	.005	0.991	0.981, 1.000
γ -glutamyl transpeptidase level*	935	.154	0.994	0.981, 1.007
Lactate dehydrogenase level†	937	.143	0.993	0.978, 1.007
γ -globulin level †	118	.225	0.996	0.985, 1.006
Blood urea nitrogen level	968	.098	0.977	0.938, 1.018
Serum creatinine level	971	.926	0.967	0.333, 2.807
Total cholesterol level†	553	<.001	1.139	1.047, 1.240
PT time	780	.262	0.993	0.975, 1.011
Child-Pugh classification (overall)	1203	<.001
Child-Pugh class A	980	...	Reference	...
Child-Pugh class B (vs class A)	209	<.001	0.340	0.209, 0.556
Child-Pugh class C (vs class A)	14	<.001	0.056	0.008, 0.393
ICG-R15	128	.142	0.977	0.932, 1.024

Note.—“Reference” indicates the category used as the reference value.

* Significance level: $P < .05/16 = .003125$.

† Odds ratio for a 10-unit increase.

Table 4

Results of Multiple Logistic Regression Analyses for Biochemical Factors in 534 Patients, Including Child-Pugh Classification

Variable	<i>P</i> Value	Odds Ratio*	95% CI
AST level*	.081	0.955	0.907, 1.006
Total bilirubin level	.020	0.779	0.631, 0.962
PT activity*	.001	1.271	1.109, 1.455
Total cholesterol level*	.005	1.088	1.025, 1.155
Child-Pugh class			
Class A	...	Reference	...
Class B and C	.067	0.558	0.299, 1.041

Note.—“Reference” indicates the category used as the reference value.

* Odds ratio for a 10-unit increase.

The time-LSC curve of group A was consistently higher than that of group B ($P < .001$ at all time points) at a significance level of .0125 (Fig 1, Appendix E4 [online]). The lower limit of two-sided 95% CIs of estimated LSC mean was over 1.5 for group A at 10 minutes (Fig 1, Table 5). The percentages of patients in group A who achieved a level

of LSC of at least 1.5 at 15 minutes and at 20 minutes were 81.2% (95% CI: 76.8%, 85.0%) and 88.7% (95% CI: 85.9%, 91.0%), respectively, whereas only 67.5% (95% CI: 63.5%, 71.3%) of those in group B achieved the level at 20 minutes.

In nine patients who could not obtain satisfactory liver enhancement

(LSC ≥ 1.5) within 20 minutes, further hepatobiliary imaging was performed at 22–95 minutes (median, 23 minutes); nevertheless, all of them failed to achieve satisfactory liver enhancement (range, 0.96–1.46).

Comparison of LSC between 1.5-T and 3.0-T MR Imaging

LSC data obtained at 1.5 T (1056 patients) and 3.0 T (697 patients) were analyzed in 1753 patients. The test of fixed effects showed no interaction between time and groups ($P = .368$). No significant difference in LSC values was observed between 1.5-T and 3.0-T MR imaging ($P = .280$), whereas LSC was significantly increased in both of the groups at 20 minutes ($P < .001$) at a significance level of less than .00625. Details of this analysis are presented in Appendix E4 (online).

Relationship between LSC at 20 Minutes and HBV and HCV

Among 1241 patients whose LSC data were available at 20 minutes, 692 patients had HBV or HCV. Satisfactory liver enhancement (LSC ≥ 1.5) was seen in 174 (84.9%) of 205 patients with HBV and in 336 (69.0%) of 487 patients with HCV (Appendix E5 [online]).

Satisfactory liver enhancement at 20 minutes was significantly less likely to be achieved by patients with HCV than those with HBV (odds ratio, 0.440; 95% CI: 0.284, 0.680; $P < .001$; Appendix E5 [online]).

Relationship between Satisfactory Liver Enhancement at 20 Minutes and HCC and Liver Metastasis

Our study included 1085 patients who underwent MR imaging for HCC or for liver metastasis, whose LSC data were available at 20 minutes. Satisfactory liver enhancement (LSC ≥ 1.5) was seen in 192 (90.1%) of 213 patients with liver metastasis and in 648 (74.3%) of 872 patients with HCC (Appendix E5 [online]). Satisfactory liver enhancement at 20 minutes was significantly less likely to be achieved by patients with HCC than in those with liver metastasis (odds ratio, 0.323; 95% CI:

Figure 1

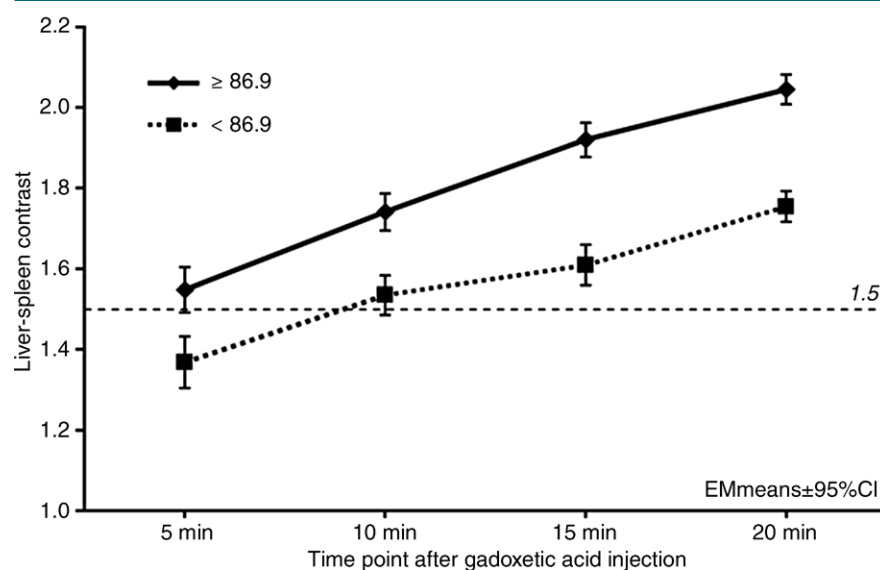


Figure 1: Graph shows the comparison of LSC between each time point. The cutoff value of PT activity was set at 86.9% from receiver operating characteristic analysis. The lower limit of the two-sided 95% CI for PT activity of at least 86.9% (group A, estimated marginal [EM] means, 1.741; standard error, 0.023; two-sided 95% CI: 1.695, 1.787) was over 1.5 for LSC at 10 minutes, whereas that for PT activity less than 86.9% (group B, mean, 1.609; standard error, 0.026; 95% CI: 1.559, 1.660) was over 1.5 for LSC at 15 minutes.

Table 5

Comparison of LSC at Each Time Point for PT Activity of at Least 86.9% and PT Activity Less Than 86.9%

Group and Time Point	No. of Eligible Patients	Estimated Marginal Mean	Standard Error	Two-sided 95% CI
Group A, PT activity $\geq 86.9\%$				
5 min	128	1.548	0.029	1.492, 1.604
10 min	236	1.741	0.023	1.695, 1.787
15 min	377	1.920	0.022	1.878, 1.962
20 min	626	2.045	0.019	2.008, 2.081
Group B, PT activity $< 86.9\%$				
5 min	96	1.368	0.033	1.304, 1.432
10 min	208	1.535	0.025	1.485, 1.584
15 min	256	1.609	0.026	1.559, 1.660
20 min	575	1.754	0.020	1.716, 1.793

Note.—LSC was consistently higher in group A than in group B and increased consistently in both groups (details appear in Appendix E4 [online]).

0.199, 0.524; $P < .001$; Appendix E5 [online]).

LLC Values

Nine hundred eighty-six of 988 registered hepatic tumors could be analyzed for LLC (data not available for two lesions). The mean size of hepatic lesions

measured at 20 minutes was 2.3 cm (range, 0.3–27.0 cm). The total valid number of tumors in five hepatic diagnostic categories evaluated was 892 (HCC, 478 [53.6%]; liver metastasis, 189 [21.2%]; borderline lesion, 49 [5.5%]; liver cyst, 66 [7.4%]; and liver hemangioma, 110 [12.3%]; Table 6).

The tests of fixed effects in the mixed-effects model showed significant interaction between time and five diagnostic categories ($P = .018$, Appendix E6 [online]). Details of this analysis are presented in Appendix E6 (online). LLC was significantly higher in HCC (Fig 2) than in liver metastasis (Fig 3) at all time points ($P < .0001$) and was significantly lower than that of borderline lesions at 5 minutes ($P = .0002$) and 10–20 minutes ($P < .0001$) at a significance level of less than .00125 (Appendix E6, Appendix E7 [online]).

When subgroup analysis was performed for patients with LSC less than 1.5, the PT activity group changed the LLC of borderline lesions from a mean value of 0.909 (standard error, 0.134; 95% CI: 0.612, 1.206) in PT activity of at least 86.9% to a mean value of 0.999 (standard error, 0.113; 95% CI: 0.748, 1.250) in PT activity less than 86.9% at 20 minutes (not statistically significant).

Comparison of LLC between 1.5-T and 3.0-T MR Imaging

LLC data obtained with 1.5-T and 3.0-T MR imaging were analyzed in 984 hepatic tumors (1.5 T, 527 tumors; 3.0 T, 457 tumors). The test of fixed effects showed no significant interaction between time and groups ($P = .332$). No significant difference in LLC was observed between 1.5 T and 3.0 T ($P = .133$), whereas LLC was significantly lowered in both of the groups at 20 minutes ($P < .001$). Details of this analysis are presented in Appendix E6 (online).

Discussion

Our results indicate that PT activity, total bilirubin level, and total cholesterol level are predictors of subsequent Gd-EOB-DTPA liver enhancement. In particular, PT activity is a strongly associated prediction factor of liver enhancement in the hepatobiliary phase. PT activity of at least 86.9% could be used to shorten examination times, allowing increased clinical efficiency of Gd-EOB-DTPA-enhanced MR imaging.

Strong association of PT activity with liver enhancement is easily

Table 6

Comparison of LLC at Each Time Point for Five Liver Diagnostic Categories

Diagnosis and Time Point	No. of Eligible Tumors	Estimated Marginal Mean	Standard Error	Two-sided 95% CI
HCC				
5 min	43	0.761	0.014	0.733, 0.790
10 min	107	0.712	0.011	0.691, 0.734
15 min	135	0.699	0.012	0.676, 0.722
20 min	381	0.681	0.009	0.664, 0.699
Liver metastasis				
5 min	12	0.632	0.026	0.580, 0.684
10 min	40	0.591	0.018	0.555, 0.626
15 min	77	0.536	0.017	0.502, 0.570
20 min	125	0.523	0.015	0.494, 0.552
Borderline lesion				
5 min	2	0.990	0.057	0.878, 1.102
10 min	32	0.927	0.028	0.872, 0.981
15 min	18	0.928	0.031	0.867, 0.989
20 min	42	0.898	0.027	0.845, 0.951
Liver hemangioma				
5 min	5	0.725	0.040	0.646, 0.803
10 min	18	0.647	0.029	0.591, 0.703
15 min	31	0.565	0.027	0.513, 0.618
20 min	43	0.560	0.025	0.512, 0.609
Liver cyst				
5 min	3	0.360	0.045	0.271, 0.449
10 min	67	0.361	0.019	0.324, 0.398
15 min	39	0.354	0.021	0.313, 0.396
20 min	93	0.345	0.018	0.309, 0.380

Note.—LLC was significantly higher in HCC than in liver metastasis at all time points. LLC was significantly lower in HCC than in borderline lesions at all time points (details appear in Appendix E6 [online]).

accepted because measurement of the blood coagulation factor can be used to estimate liver synthetic capacity. Results of prior studies have also shown that the liver enhancement level with Gd-EOB-DTPA is correlated with liver function level, such as AST, total bilirubin level, albumin level, ICG-R15, PT activity, and platelet count (9–11).

Organic anion-transporting polypeptide, or OATP, 1B1 transport bilirubin is a major determinant of serum bilirubin level (13–15), and OATP is also known as the transporter of Gd-EOB-DTPA into hepatocytes (16). Our result that showed a significant relationship between total bilirubin level and liver enhancement should be understood in the context of these mechanisms. According to a previous investigation (17), patients with total bilirubin level

of at least 1.8 mg/dL (30.8 μ mol/L) had lower liver and biliary enhancement than those with total bilirubin level less than 1.8 mg/dL (30.8 μ mol/L). Thus, this result of their report (17) shows a correlation equivalent to the result of our study. Genetic polymorphisms of OATP 1B1 (18) and competition from other drugs (19) are recognized as signal confounders in Gd-EOB-DTPA-enhanced MR imaging, and they are suspected of being confounders in the correlation between biochemical factors and hepatic enhancement. Further study is needed for genetic polymorphisms of OATP 1B1, a major confounder of reduced liver signal intensity in Gd-EOB-DTPA-enhanced MR imaging.

ICG-R15 is known to be an important predictor of liver enhancement

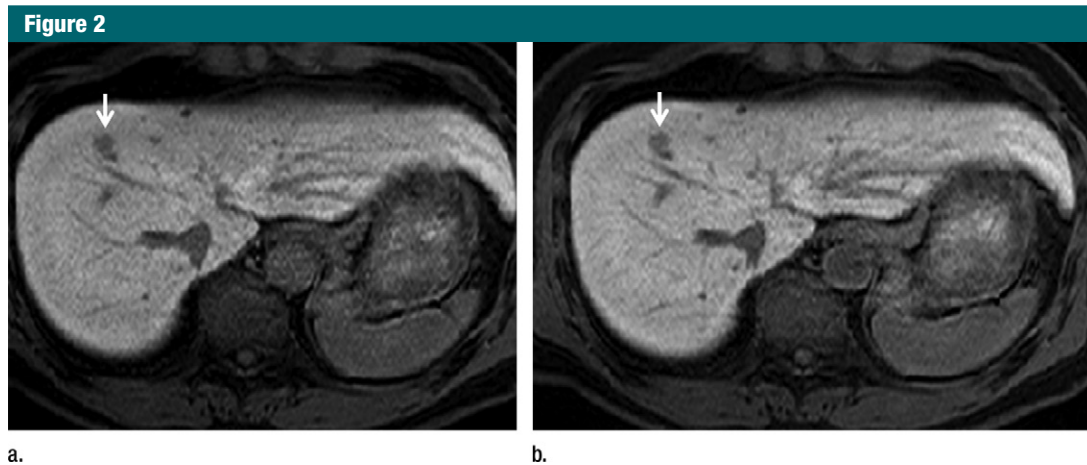


Figure 2: Axial MR images of HCC (arrow) in liver segment 8 in a 58-year-old man. Hepatobiliary phase Gd-EOB-DTPA-enhanced MR images were obtained at (a) 10 minutes and (b) 20 minutes. The LSC of HCC was 1.54 at 10 minutes (a) and 1.68 at 20 minutes (b), and the liver enhancement increased from 10 minutes to 20 minutes. The LLC of HCC was 0.67 at 10 minutes (a) and 0.63 at 20 minutes (b). Parameters related to liver function are AST level, 28 IU/L (0.47 μ kat/L); ALT level, 20 IU/L (0.3 μ kat/L); albumin level, 4.8 g/dL (48 g/L); total bilirubin level, 0.3 mg/dL (5.1 μ mol/L); PT activity, 108.9%; total protein level, 7.1 g/dL (71 g/L); alkaline phosphatase level, 211 IU/L (3.5 μ kat/L); γ -glutamyl transpeptidase level, 38 IU/L; lactate dehydrogenase level, 216 IU/L (3.6 μ kat/L); blood urea nitrogen level, 18 mg/dL (6.4 mmol/L); serum creatinine level, 0.75 mg/dL (66.3 μ mol/L); PT time, 11.3 seconds, and Child-Pugh classification A.

on Gd-EOB-DTPA-enhanced MR images; it can be used to predict satisfactory liver enhancement at 20 minutes (8,20). However, since most of our patients were not surgical candidates, the data we obtained with ICG-R15 are insufficient to analyze the relationship between liver enhancement and ICG-R15.

When LLC of each liver tumor was compared, it seemed possible to differentiate between HCC and borderline lesions because LLC of HCC was significantly lower than that of borderline lesions. Since background liver signal intensity was similar between HCCs and borderline lesions, this difference in LLC may be due to decreased but not absent uptake of Gd-EOB-DTPA in borderline lesions compared with those in HCCs in which the uptake of Gd-EOB-DTPA is markedly decreased or absent (21,22). This result of our study is similar to that in a previous report, in which low signal intensity of tumors in the hepatobiliary phase was sufficiently sensitive to differentiate definite HCC from borderline lesions (22).

There was no significant difference between LSCs at 3.0-T and 1.5-T MR imaging; this result may indicate that 3.0-T MR imaging can be used with a

performance similar to that of 1.5-T MR imaging.

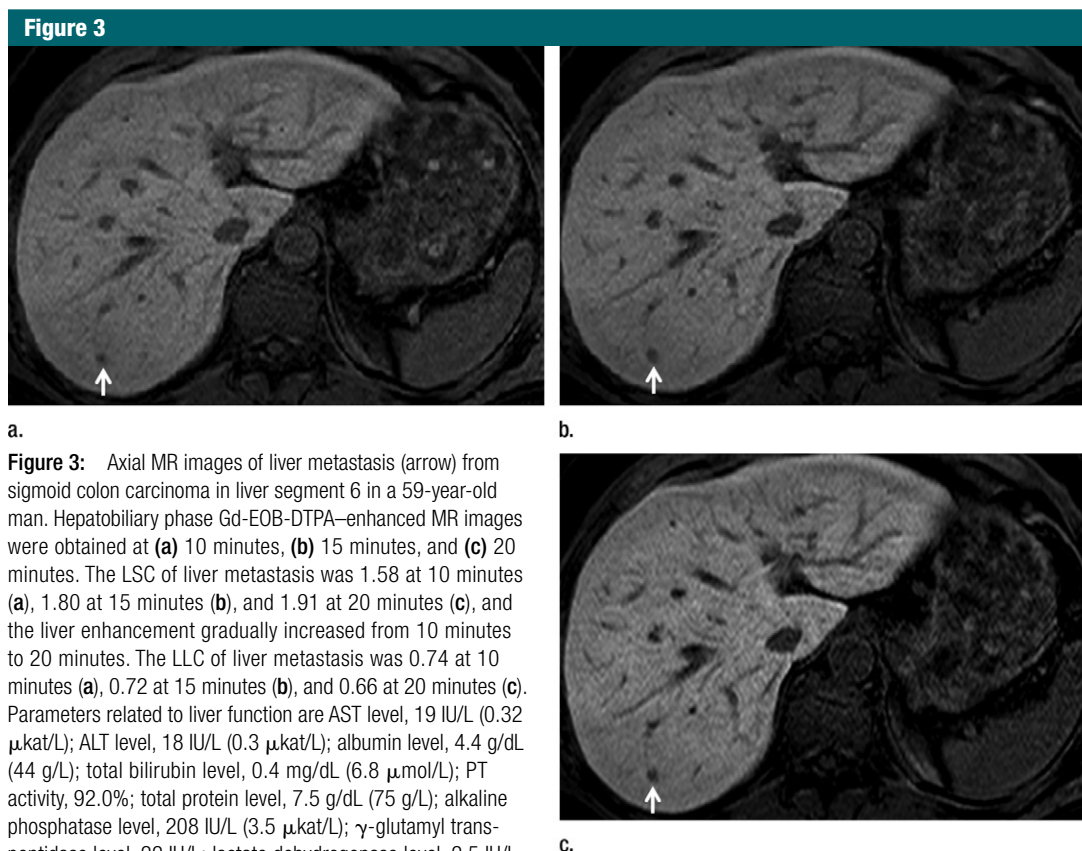
Satisfactory liver enhancement at 20 minutes was significantly more likely to be achieved (a) in patients with HBV than in those with HCV and (b) in patients with liver metastasis than in those with HCC. These findings are probably due to less advanced stage of liver cirrhosis in patients with HCC and HBV than in those with HCV. These results can provide estimations of liver enhancement level before Gd-EOB-DTPA-enhanced MR imaging.

Knowing the optimal imaging time point in the hepatobiliary phase is important. Many of the hospitals needed 20 minutes to be able to acquire images in the hepatobiliary phase, and LLC at 20 minutes was significantly lower than at 5–10 minutes. But, it may be possible to shorten examination times with LSC of at least 1.5 when patients have PT activity of at least 86.9%.

Our study had some limitations. First, ICG-R15 data might not be enough to analyze the relationship between liver enhancement and ICG-R15. However, measuring ICG-R15 requires greater care relative to PT activity. The second limitation is that there were various

MR imaging methods used in this non-interventional study conducted at many hospitals. Therefore, imaging parameters varied, and this may have affected quantitative signal intensity of liver and tumors. However, we all used the three-dimensional T1-weighted technique, so the effect could be minimized. Also, the image analysis did not include the individual region of interest data for each liver tumor, although we know the range of region of interest diameters. Third, there were diagnostic limitations of the differentiation of HCC and borderline lesions without pathologic findings because of the imaging overlap. But, we believe that a certain accuracy level of diagnosis was accomplished as in previous reports (23–25). Fourth, the thresholds identified have not been tested independently with a validation data set.

Signal intensity analysis may be used to achieve a useful outcome in collected lots of data on liver and tumor enhancement. But, T1 relaxometry (measuring T1 values) should be investigated for liver and tumor enhancement in the future, because quantitative T1 relaxometry offers promising prospects for the estimation of liver function (5,26,27).



a.

b.

c.

Figure 3: Axial MR images of liver metastasis (arrow) from sigmoid colon carcinoma in liver segment 6 in a 59-year-old man. Hepatobiliary phase Gd-EOB-DTPA-enhanced MR images were obtained at (a) 10 minutes, (b) 15 minutes, and (c) 20 minutes. The LSC of liver metastasis was 1.58 at 10 minutes (a), 1.80 at 15 minutes (b), and 1.91 at 20 minutes (c), and the liver enhancement gradually increased from 10 minutes to 20 minutes. The LLC of liver metastasis was 0.74 at 10 minutes (a), 0.72 at 15 minutes (b), and 0.66 at 20 minutes (c). Parameters related to liver function are AST level, 19 IU/L (0.32 μ kat/L); ALT level, 18 IU/L (0.3 μ kat/L); albumin level, 4.4 g/dL (44 g/L); total bilirubin level, 0.4 mg/dL (6.8 μ mol/L); PT activity, 92.0%; total protein level, 7.5 g/dL (75 g/L); alkaline phosphatase level, 208 IU/L (3.5 μ kat/L); γ -glutamyl transpeptidase level, 22 IU/L; lactate dehydrogenase level, 2.5 IU/L (μ kat/L); blood urea nitrogen level, 13 mg/dL (4.6 mmol/L); serum creatinine level, 0.68 mg/dL (60.1 μ mol/L); total cholesterol level, 207 mg/dL (5.36 mmol/L); PT time, 12.0 seconds; ICG-R15, 5%; and Child-Pugh classification A.

In conclusion, from the data in this large patient population, the liver enhancement in the hepatobiliary phase of Gd-EOB-DTPA-enhanced MR imaging is significantly associated with PT activity, total bilirubin level, and total cholesterol level. Knowing the PT activity cutoff value of 86.9% before the examination is useful for predicting the degree of liver enhancement and suggesting an optimal imaging time. No difference in liver enhancement was observed between the 1.5- and 3.0-T MR imaging equipment used. More satisfactory liver enhancement was obtained (a) in the patients with HBV than in those with HCV and (b) in the patients with liver metastasis than in those with HCC. The LLC in HCC, liver metastasis, and liver hemangiomas was lower than that in borderline lesions over time. In the patients with PT activity of at least 86.9% and/or liver metastasis, the examination time of the hepatobiliary

phase of Gd-EOB-DTPA-enhanced MR imaging could be shortened.

Author affiliations: Dept of Radiology, Kinki Univ Faculty of Medicine, Osaka, Japan (M.O., T.M.); Dept of Radiology, Juntendo Univ, Faculty of Medicine, Tokyo, Japan (R.K.); Dept of Diagnostic Radiology, Inst of Biomedical and Health Sciences, Hiroshima Univ, Hiroshima, Japan (Y.N.); Dept of Diagnostic Imaging and Nuclear Medicine, Kyoto Univ Graduate School of Medicine, Kyoto, Japan (H.I.); Dept of Radiology and Services, Gifu Univ Hosp, Gifu, Japan (S.G.); Dept of Radiology, School of Medicine, Fujita Health Univ, Toyoake, Japan (R.H.); Dept of Radiology, Nihon Univ School of Medicine, Tokyo, Japan (H.H.); Dept of Radiology, Faculty of Medicine, Fukuoka Univ, Fukuoka, Japan (Y.S.); Depts of Radiology (A.K.) and Advanced Medical Imaging (O.M.), Graduate School of Medical Science, Kanazawa Univ, Kanazawa, Japan; Dept of Radiology, Shinshu Univ School of Medicine, Matsumoto, Japan (Y.F.); Dept of Central Endoscopy and Ultrasound, Nara Medical Univ Hosp, Nara, Japan (N.M.); Dept of Radiology, Osaka Medical College, Takatsuki, Japan (M.Y.); Dept of Radiology, Univ of Yamanashi School of Medicine, Chuo, Japan (T.I.); Dept of Radiology, Kawasaki Medical School, Kurashiki, Japan (A.H.); Dept of

Radiology, Osaka Univ Graduate School of Medicine, Suita, Japan (M.H.); and Div of Radiology, Dept of Pathophysiological and Therapeutic Science, Faculty of Medicine, Tottori Univ, Yonago, Japan (S.F.).

Acknowledgments: Participants in this multicenter trial were drawn from radiology departments of the following institutions: Kinki University Hospital, Juntendo University Hospital, Hiroshima University Hospital, Kyoto University Hospital, Gifu University Hospital, Fujita Health University Hospital, Nihon University Itabashi Hospital, Fukuoka University Hospital, Kanazawa University Hospital, Shinshu University Hospital, Nara Medical University Hospital, Osaka Medical College Hospital, University of Yamanashi Hospital, Kawasaki Medical School Hospital, Osaka University Hospital, Tottori University Hospital, Hokkaido University Hospital, Toho University Omori Medical Center, Wakayama Medical University Hospital, University of Miyazaki Hospital, Jichi Medical University Hospital, Nihon Medical School Chiba Hokusoh Hospital, Cancer Institute Hospital of JFCR, Saitama Medical University Saitama Medical Center, Juntendo University Nerima Hospital, Osaka Medical Center for Cancer and Cardiovascular Diseases, Tokyo Medical University Ibaraki Medical Center, Gunma University Hos-

pital, Saitama Medical University International Medical Center, Kagoshima University Medical and Dental Hospital, Niigata University Medical and Dental Hospital, Dokkyo Medical University Koshigaya Hospital, Saitama Medical University Hospital, Oita University Hospital, Juntendo University Urayasu Hospital, Jikei University Kashiwa Hospital, Jikei University Katsushika Medical Center, Kyushu Cancer Center, Shikoku Cancer Center, Nagasaki Medical Center, Kurume University Hospital, Nagasaki University Hospital, Shimane University Hospital, The Institute of Medical Science the University of Tokyo, and Tokyo Women's Medical University Yachiyo Medical Center. All institutions are located in Japan. We thank Hirotsugu Yasuda (Data Research Section, Kondo P.P.) for statistical analysis.

Disclosures of Conflicts of Interest: M.O. disclosed no relevant relationships. T.M. disclosed no relevant relationships. R.K. disclosed no relevant relationships. Y.N. disclosed no relevant relationships. H.I. disclosed no relevant relationships. S.G. disclosed no relevant relationships. R.H. disclosed no relevant relationships. H.H. disclosed no relevant relationships. Y.S. disclosed no relevant relationships. A.K. disclosed no relevant relationships. Y.F. disclosed no relevant relationships. N.M. disclosed no relevant relationships. M.Y. disclosed no relevant relationships. T.I. disclosed no relevant relationships. A.H. disclosed no relevant relationships. M.H. disclosed no relevant relationships. S.F. disclosed no relevant relationships. O.M. Activities related to the present article: disclosed no relevant relationships. Activities not related to the present article: author received payment from Bayer for educational lectures. Other relationships: disclosed no relevant relationships.

References

- Bluemke DA, Sahani D, Amendola M, et al. Efficacy and safety of MR imaging with liver-specific contrast agent: U.S. multicenter phase III study. *Radiology* 2005;237(1):89–98.
- Hamm B, Staks T, Mühler A, et al. Phase I clinical evaluation of Gd-EOB-DTPA as a hepatobiliary MR contrast agent: safety, pharmacokinetics, and MR imaging. *Radiology* 1995;195(3):785–792.
- Huppertz A, Haraida S, Kraus A, et al. Enhancement of focal liver lesions at gadoxetic acid-enhanced MR imaging: correlation with histopathologic findings and spiral CT—initial observations. *Radiology* 2005;234(2):468–478.
- Tsuda N, Okada M, Murakami T. Potential of gadolinium-ethoxybenzyl-diethylenetriamine pentaacetic acid (Gd-EOB-DTPA) for differential diagnosis of nonalcoholic steatohepatitis and fatty liver in rats using magnetic resonance imaging. *Invest Radiol* 2007;42(4):242–247.
- Katsube T, Okada M, Kumano S, et al. Estimation of liver function using T1 mapping on Gd-EOB-DTPA-enhanced magnetic resonance imaging. *Invest Radiol* 2011;46(4):277–283.
- Katsube T, Okada M, Kumano S, et al. Estimation of liver function using T2* mapping on gadolinium ethoxybenzyl diethylenetriamine pentaacetic acid enhanced magnetic resonance imaging. *Eur J Radiol* 2012;81(7):1460–1464. [Published correction appears in *Eur J Radiol* 2013;82(6):1039.]
- Kim T, Murakami T, Hasuiki Y, et al. Experimental hepatic dysfunction: evaluation by MRI with Gd-EOB-DTPA. *J Magn Reson Imaging* 1997;7(4):683–688.
- Motosugi U, Ichikawa T, Sou H, et al. Liver parenchymal enhancement of hepatocyte-phase images in Gd-EOB-DTPA-enhanced MR imaging: which biological markers of the liver function affect the enhancement? *J Magn Reson Imaging* 2009;30(5):1042–1046.
- Kim HY, Choi JY, Park CH, et al. Clinical factors predictive of insufficient liver enhancement on the hepatocyte-phase of Gd-EOB-DTPA-enhanced magnetic resonance imaging in patients with liver cirrhosis. *J Gastroenterol* 2013;48(10):1180–1187.
- Matsushima S, Sato Y, Yamaura H, et al. Visualization of liver uptake function using the uptake contrast-enhanced ratio in hepatobiliary phase imaging. *Magn Reson Imaging* 2014;32(6):654–659.
- Higaki A, Tamada T, Sone T, et al. Potential clinical factors affecting hepatobiliary enhancement at Gd-EOB-DTPA-enhanced MR imaging. *Magn Reson Imaging* 2012;30(5):689–693.
- Bruix J, Sherman M; American Association for the Study of Liver Diseases. Management of hepatocellular carcinoma: an update. *Hepatology* 2011;53(3):1020–1022.
- Zhang W, He YJ, Gan Z, et al. OATP1B1 polymorphism is a major determinant of serum bilirubin level but not associated with rifampicin-mediated bilirubin elevation. *Clin Exp Pharmacol Physiol* 2007;34(12):1240–1244.
- Hagenbuch B, Gui C. Xenobiotic transporters of the human organic anion transporting polypeptides (OATP) family. *Xenobiotica* 2008;38(7-8):778–801.
- König J, Seithel A, Gradhand U, Fromm MF. Pharmacogenomics of human OATP transporters. *Naunyn Schmiedeberg Arch Pharmacol* 2006;372(6):432–443.
- Narita M, Hatano E, Arizono S, et al. Expression of OATP1B3 determines uptake of Gd-EOB-DTPA in hepatocellular carcinoma. *J Gastroenterol* 2009;44(7):793–798.
- Okada M, Ishii K, Numata K, et al. Can the biliary enhancement of Gd-EOB-DTPA predict the degree of liver function? *Hepatobiliary Pancreat Dis Int* 2012;11(3):307–313.
- Nassif A, Jia J, Keiser M, et al. Visualization of hepatic uptake transporter function in healthy subjects by using gadoxetic acid-enhanced MR imaging. *Radiology* 2012;264(3):741–750.
- Ieiri I, Higuchi S, Sugiyama Y. Genetic polymorphisms of uptake (OATP1B1, 1B3) and efflux (MRP2, BCRP) transporters: implications for inter-individual differences in the pharmacokinetics and pharmacodynamics of statins and other clinically relevant drugs. *Expert Opin Drug Metab Toxicol* 2009;5(7):703–729.
- Ryeom HK, Kim SH, Kim JY, et al. Quantitative evaluation of liver function with MRI using Gd-EOB-DTPA. *Korean J Radiol* 2004;5(4):231–239.
- Sano K, Ichikawa T, Motosugi U, et al. Imaging study of early hepatocellular carcinoma: usefulness of gadoxetic acid-enhanced MR imaging. *Radiology* 2011;261(3):834–844.
- Kitao A, Matsui O, Yoneda N, et al. The uptake transporter OATP8 expression decreases during multistep hepatocarcinogenesis: correlation with gadoxetic acid enhanced MR imaging. *Eur Radiol* 2011;21(10):2056–2066.
- Hayashi M, Matsui O, Ueda K, et al. Correlation between the blood supply and grade of malignancy of hepatocellular nodules associated with liver cirrhosis: evaluation by CT during intraarterial injection of contrast medium. *AJR Am J Roentgenol* 1999;172(4):969–976.
- Muhi A, Ichikawa T, Motosugi U, et al. High-b-value diffusion-weighted MR imaging of hepatocellular lesions: estimation of grade of malignancy of hepatocellular carcinoma. *J Magn Reson Imaging* 2009;30(5):1005–1011.
- Nasu K, Kuroki Y, Tsukamoto T, Nakajima H, Mori K, Minami M. Diffusion-weighted imaging of surgically resected hepatocellular carcinoma: imaging characteristics and relationship among signal intensity, apparent diffusion coefficient, and histopathologic grade. *AJR Am J Roentgenol* 2009;193(2):438–444.
- Ding Y, Rao SX, Chen C, Li R, Zeng MS. Assessing liver function in patients with HBV-related HCC: a comparison of T1 mapping on Gd-EOB-DTPA-enhanced MR imaging with DWI. *Eur Radiol* 2015;25(5):1392–1398.
- Onoda M, Hyodo T, Murakami T, et al. Optimizing signal intensity correction during evaluation of hepatic parenchymal enhancement on gadoxetate disodium-enhanced MRI: comparison of three methods. *Eur J Radiol* 2015;84(3):339–345.